




## Article

# Development of Poly(L-Lactic Acid)/Chitosan/Basil Oil Active Packaging Films via a Melt-Extrusion Process Using Novel Chitosan/Basil Oil Blends

Constantinos E. Salmas <sup>1,\*</sup> , Aris E. Giannakas <sup>2,\*</sup> , Maria Baikousi <sup>1</sup>, Areti Leontiou <sup>3</sup>, Zoe Siasou <sup>2</sup> and Michael A. Karakassides <sup>1,4</sup> 

<sup>1</sup> Department of Materials Science and Engineering, University of Ioannina, 45110 Ioannina, Greece; mariabaikousi@gmail.com (M.B.); mkarakas@uoi.gr (M.A.K.)

<sup>2</sup> Department of Food Science and Technology, University of Patras, 30100 Agrinio, Greece; zoesiasou@gmail.com

<sup>3</sup> Department of Business Administration of Food and Agricultural Enterprises, University of Patras, 30100 Agrinio, Greece; aleontiu@upatras.gr

<sup>4</sup> Institute of Materials Science and Computing, University Research Center of Ioannina (URCI), 45110 Ioannina, Greece

\* Correspondence: ksalmas@uoi.gr (C.E.S.); agiannakas@upatras.gr (A.E.G.)

**Abstract:** Following the global trend toward a cyclic economy, the development of a fully biodegradable active packaging film is the target of this work. An innovative process to improve the mechanical, antioxidant, and barrier properties of Poly(L-Lactic Acid)/Chitosan films is presented using essential basil oil extract. A Chitosan/Basil oil blend was prepared via a green evaporation/adsorption method as a precursor for the development of the Poly(L-Lactic Acid)/Chitosan/Basil Oil active packaging film. This Chitosan/Basil Oil blend was incorporated directly in the Poly(L-Lactic Acid) matrix with various concentrations. Modification of the chitosan with the Basil Oil improves the blending with the Poly(L-Lactic Acid) matrix via a melt-extrusion process. The obtained Poly(L-Lactic Acid)/Chitosan/Basil Oil composite films exhibited advanced food packaging properties compared to those of the Poly(L-Lactic Acid)/Chitosan films without Basil Oil addition. The films with 5%wt and 10%wt Chitosan/Basil Oil loadings exhibited better thermal, mechanical, and barrier behavior and significant antioxidant activity. Thus, PLLA/CS/BO5 and PLLA/CS/BO10 are the most promising films to potentially be used for active packaging applications.

**Keywords:** PLLA; chitosan; basil oil; active packaging; films; barrier properties; antioxidant properties



**Citation:** Salmas, C.E.; Giannakas, A.E.; Baikousi, M.; Leontiou, A.; Siasou, Z.; Karakassides, M.A. Development of Poly(L-Lactic Acid)/Chitosan/Basil Oil Active Packaging Films via a Melt-Extrusion Process Using Novel Chitosan/Basil Oil Blends. *Processes* **2021**, *9*, 88. <https://doi.org/10.3390/pr9010088>

Received: 18 December 2020

Accepted: 29 December 2020

Published: 3 January 2021

**Publisher's Note:** MDPI stays neutral with regard to jurisdictional claims in published maps and institutional affiliations.



**Copyright:** © 2021 by the authors. Licensee MDPI, Basel, Switzerland. This article is an open access article distributed under the terms and conditions of the Creative Commons Attribution (CC BY) license (<https://creativecommons.org/licenses/by/4.0/>).

## 1. Introduction

Nowadays, the global trend towards a cyclic economy, sustainability, green economy, and nanotechnology suggests the use of by-products, biomass, and/or bio-wastes which have zero environmental fingerprints as raw materials for the development of novel biodegradable active packaging materials. One of the most promising and widely used bio-based polymers which has already been commercialized, is Poly(L-Lactic Acid) (PLLA). PLLA is produced by the polymerization of the L-Lactic Acid monomer, which is produced through fermentation of sugars. Such sugars are extracted from biomass sources (e.g., corn starch, tapioca, sugar cane, or sugar beet) [1,2]. Compared with petroleum-based polymer production, the PLLA production process requires about 50% less energy consumption [3]. Moreover, PLLA is not only bio-based but also compostable and biodegradable through hydrolysis by microorganisms [4]. Thus, PLLA could be a green alternative to some common thermoplastic polymers such as polyethylene (PE), polypropylene (PP), polystyrene (PS), and polyethylene terephthalate (PET) [5,6]. Its mechanical properties make this polymer suitable for use in various production processes. However, its high elastic modulus makes its plastic deformation limited, and thus, it becomes brittle.

Chitosan (CS) is another biopolymer promising for food packaging applications. CS is a linear polysaccharide that is produced by treating a food by-product, i.e., the chitin shells of crustaceans [7]. CS exhibits high barrier values, significant antioxidant properties, and antimicrobial activity. Such properties give this material great potential for use as packaging material [8]. The main disadvantages of CS are the weak tensile properties and the disability to blend in extruders with other materials that are commonly used in the industry for packaging film production.

Researchers developed composite membranes to overcome the disadvantages of various biopolymers. Blending Poly(L-Lactic Acid) (PLLA) with CS to produce a composite membrane is an attractive procedure for the production of new polymeric materials with controlled properties [9–15]. One more advantage of the polymer blending procedure is the production of materials exhibiting versatility, simplicity, and cost-effectiveness. The physicochemical and mechanical properties of the material which is produced after blending are dependent on the state of the mixture (i.e., solid or liquid) and the miscibility of the components.

On the other hand, the recent trend in food production processes is the development of active/bioactive packaging films using the advantages of nanotechnology [16–19]. In this way, researchers are using various methods to intrude natural antioxidants, such as essential oils [16] or natural extracts [19], in packaging films. The replacement of synthetic antioxidants (e.g., butyl-hydroxytoluene (BHT), butyl-hydroxyanisole (BHA), and tert-butyl hydroxyquinone (TBHQ) which exhibit bad effects on consumers health) with natural antioxidants in active/bioactive packaging films enhances the shelf-life of food and increases the positive environmental fingerprint.

The novel biodegradable composite active packaging film developed during this work was made with (1) PLLA, (2) CS, and (3) Basil essential Oil (BO). Modification of CS with BO via an easy green method before mixing with PLLA was the main innovation of the proposed process. This modification led to a CS/BO blend. Sequentially, this novel CS/BO blend was mixed with the PLLA polymeric matrix in four different %w/w concentrations (i.e., 5, 10, 20, and 30%w/w) and melt-extruded. The CS/BO blend and all the PLLA/CS/BO active packaging films were characterized via various techniques. More specifically, parameters such as tensile properties, water and oxygen barrier properties, water sorption, and antioxidant activity were measured for the obtained packaging films.

## 2. Materials and Methods

### 2.1. Materials

PLLA was supplied by NatureWorks, Minnetonka, MN, US, with the trade name Ingeo™ Biopolymer 3052D. CS with medium molecular weight and deacetylation degree at 90% was supplied from Flurochem, Hadfield, Derbyshire, United Kingdom (cat. no. FCB051814). Basil essential oil (BO) was purchased from Esperis spa., Binda, Milano, Italy and according to the attached safety data sheets, the % mass composition was 70–80% estragole, 7.5–10% linalool, 1–3% eucalyptol, 0.5–1.0% eugenol, and 0.5–1.0% D-limonene.

### 2.2. Preparation Methods

#### 2.2.1. Preparation of CS/BO Hybrid Blend

The CS/BO blend was prepared according to the adsorption/evaporation process which is described in our previous publication [20]. Briefly, 5 g of CS was spread in an aluminum beaker. A small quartz beaker was placed in the middle of the aluminum beaker and was filled with 5 g of BO. The whole “apparatus” was sealed and put in an oven at 130 °C for 24 h. Under these conditions, the volatile components of the BO were evaporated and adsorbed into the CS. Following this innovative preparation method, we successfully encapsulated the most volatile, the most active, and the less toxic fraction of extraction oils. The obtained CS/BO hybrid blend could be easily mixed as a component for active packaging film production.

### 2.2.2. Preparation of PLLA/CS/BO Films

PLLA/CS/BO films of 300–350  $\mu\text{m}$  average thickness were developed by the melt-mixing method (see Figure 1) using a minilab twin co-rotating extruder (D516 mm, L/D524). PLLA/CS films were also prepared for comparison reasons. PLLA pellets were dried in an oven under vacuum at 98 °C for 2 h before their use. For 5 min of total melt process time, the temperature was kept stable at 170 °C, and the screw rotation speed was 100 rpm. Samples were prepared by the addition of the CS/BO hybrid blend into PLLA. The CS/BO blend composition was fixed at 5, 10, 20, and 30% *w/w*. Different samples were also prepared by the addition of pure CS into PLLA with the same previous compositions. The melted strands were exported from the extruder machine and cut into small granules with a granulated machine. Films were produced using a hydraulic press with heated platens. Hot-pressing of approximately 1 g of the obtained granules at 110 °C under 2.0 MPa constant pressure for 3 min provided the final product. These products were kept in a desiccator under 25 °C temperature and relative humidity of 50% RH. Finally, for comparison reasons, a “blank” film of PLLA without the addition of pure CS or CS/BO was also prepared following the same procedure. The code names of all samples are listed in Table 1. The amount of PLLA and CS/BO used in the preparation stage of the PLLA/CS/BO active films as well as the process conditions at the melting extrusion stage are listed in Table 1.



**Figure 1.** Scheme with the extrusion process used for the preparation of Poly(L-Lactic Acid) (PLLA)/chitosan (CS) and PLLA/CS/BO composites films: (a) “blank” PLLA, (b) PLLA/CS/BO5, (c) PLLA/CS/BO10, (d) PLLA/CS/BO20, and (e) PLLA/CS/BO30.

### 2.3. XRD Analysis

The morphological evaluation of the PLLA/CS and PLLA/CS/BO films was investigated via XRD patterns obtained using a Brüker D8 Advance X-ray diffractometer (Bruker, Analytical Instruments, S.A., Athens, Greece) equipped with a LINXEYE XE High-Resolution Energy-Dispersive detector. Typical scanning parameters were set as follows: two theta range 2–30°, increment 0.03°, and PSD 0.764.

**Table 1.** Code names, amounts of PLLA and CS/BO used, and extrusion processing conditions for all prepared active films.

| Code Name    | PLLA(g) | CS (g) | CS/BO (g) | Extruder Temperature (°C) | Extruder Rotation Speed (rpm) | Extruder Total Processing Time (min) |
|--------------|---------|--------|-----------|---------------------------|-------------------------------|--------------------------------------|
| PLLA         | 5.00    | -      | -         | 170                       | 150                           | 5                                    |
| PLLA/CS5     | 4.75    | 0.25   | -         | 170                       | 150                           | 5                                    |
| PLLA/CS10    | 4.50    | 0.50   | -         | 170                       | 150                           | 5                                    |
| PLLA/CS20    | 3.00    | 1.00   | -         | 170                       | 150                           | 5                                    |
| PLLA/CS30    | 3.50    | 1.50   | -         | 170                       | 150                           | 5                                    |
| PLLA/CS/BO5  | 4.75    | -      | 0.25      | 170                       | 150                           | 5                                    |
| PLLA/CS/BO10 | 4.50    | -      | 0.50      | 170                       | 150                           | 5                                    |
| PLLA/CS/BO20 | 3.00    | -      | 1.00      | 170                       | 150                           | 5                                    |
| PLLA/CS/BO30 | 3.50    | -      | 1.50      | 170                       | 150                           | 5                                    |

#### 2.4. FT-IR Spectrometry

The chemical structure of the PLLA/CS and PLLA/CS/BO films were investigated via IR spectra measurements. Infrared (FT-IR) spectra, which were the average of 32 scans at  $2\text{ cm}^{-1}$  resolution, were measured using an FT/IR-6000 JASCO Fourier transform spectrometer (JASCO, Interlab, S.A., Athens, Greece). Scans were carried out in the frequency range  $4000\text{--}400\text{ cm}^{-1}$ .

#### 2.5. Thermogravimetric/Differential Thermal Analysis (TG-DTA)

Thermogravimetric (TGA) and differential thermal analysis (DTA) measurements were performed on PLLA/CS/BO samples. The results were compared with the same type of measurements on PLLA/CS samples. A Perkin-Elmer Pyris Diamond TGA/DTA instrument (Interlab, S.A., Athens, Greece) was used for such measurements. Samples of approximately 5 mg were heated under nitrogen atmosphere from 25 to  $700\text{ }^{\circ}\text{C}$  and with an increasing temperature rate of  $5\text{ }^{\circ}\text{C}/\text{min}$ .

#### 2.6. Tensile Properties

Tensile measurements were carried out according to the ASTM D638 method on PLLA/CS and PLLA/CS/BO films as well as on a “blank” PLLA film (used for comparison reasons). Measurements were performed using a Simantzü AX-G 5kNt instrument (Simantzü. Asteriadis, S.A., Athens, Greece). Three to five samples of each film were tensioned at an across head speed of  $2\text{ mm}/\text{min}$ . The samples were cut in dumb-bell shape with gauge dimensions of  $10\text{ mm} \times 3\text{ mm} \times 0.22\text{ mm}$ . Force (N) and deformation (mm) were recorded during the test. Stress, strain, and modulus of elasticity were calculated based on these measurements and the gauge dimensions.

#### 2.7. Water Sorption

Films were cut into small pieces ( $12\text{ mm} \times 12\text{ mm}$ ), desiccated overnight under vacuum, and weighed to determine their dry mass. The weighed films were placed in closed beakers containing 30 mL of water ( $\text{pH} = 7$ ) and stored at  $T = 25\text{ }^{\circ}\text{C}$ . The sorption versus time plots were developed by periodical weighting of the samples until equilibrium was reached and according to the following equation:

$$\text{W.S. (\%)} = (m_{\text{Wet}} \times m_{\text{Dry}}) / m_{\text{Dry}} \times 100 \quad (1)$$

where  $m_{\text{Wet}}$  and  $m_{\text{Dry}}$  are the weights of the wet and dry films, respectively, and W.S. is the water sorption.

### 2.8. Water Vapor Permeability (WVTR)

Water vapor permeability of the PLLA/CS/BO films as well as of the “blank” PLLA film were determined at 38 °C and 50% RH according to the ASTM E96/E 96M-05 method. Measurements were carried out using a handmade apparatus and following the methodology described extensively in our previous publications [21–23].

### 2.9. Oxygen Permeability (OP)

The Oxygen Transition Rates (OTRs) of the PLLA/CS/BO films as well as of the “blank” PLLA film were measured using an oxygen permeation analyzer (8001, Systech Illinois Instruments Co., Johnsbury, IL, USA). Tests were carried out at 23 °C and 0% RH according to the ASTM D 3985 method. OTR values were measured in cc O<sub>2</sub>/m<sup>2</sup>/day. The OP values of the tested samples were calculated by multiplying the OTR values with the average film thickness, which was approximately 300–350 µm. The mean OTR value for each kind of film resulted from the measurements of three samples.

### 2.10. Antioxidant Activity

The antioxidant activity of films was evaluated using 500 mg of small pieces (approximately 3 mm × 3 mm) of each film. The sample was placed in a dark-colored glass bottle with a plastic screw cap and filled with 10 mL of DPPH ethanolic solution at 50 ppm concentration. After incubation for 24 h at 25 °C in darkness, the % antioxidant activity of the films was calculated according to Equation (2):

$$\% \text{ Antioxidant activity} = (\text{Abs}_{\text{control}} - \text{Abs}_{\text{sample}}) / \text{Abs}_{\text{control}} \times 100 \quad (2)$$

### 2.11. Statistical Analysis

All measurements were carried out measuring three samples at least for each kind of film. The statistical analysis was performed using the Statistical Software SPSS 20 for windows (SPSS Inc., Chicago, IL, USA). The results for mean values and standard deviation are presented below in Tables 2 and 3. A detailed discussion for the statistical analysis is presented in the Results section.

**Table 2.** Modulus of elasticity (E), tensile strength ( $\sigma_{\text{uts}}$ ), and % elongation at break ( $\epsilon_b$ ) of all the tested PLLA/CS and PLLA/CS/Basil essential Oil (BO) films as well as the “blank” PLLA film.

| Code Name    | Tensile E<br>(St. Dev.)<br>(MPa) | $\sigma_{\text{uts}}$ (MPa)<br>(St. Dev.) | % $\epsilon$<br>(St. Dev.) |
|--------------|----------------------------------|---|----------------------------|
| PLLA         | 2891.3(61.9)                     | 33.9(4.9)                                 | 1.4(0.5)                   |
| PLLA/CS5     | 2877.3(125.3)                    | 32.2(5.4)                                 | 1.3(0.3)                   |
| PLLA/CS10    | 2557.5(137.8)                    | 28.2(6.0)                                 | 1.1(0.3)                   |
| PLLA/CS20    | 2006.3(225.4)                    | 16.1(6.3)                                 | 0.8(0.2)                   |
| PLLA/CS30    | 1446.7(298.5)                    | 6.1(2.4)                                  | 0.5(0.1)                   |
| PLLA/CS/BO5  | 2690.7(285.3)                    | 40.3(7.9)                                 | 2.0(0.4)                   |
| PLLA/CS/BO10 | 2913.4(121.7)                    | 36.3(3.7)                                 | 1.6(0.3)                   |
| PLLA/CS/BO20 | 3060.2(184.5)                    | 21.5(4.0)                                 | 0.8(0.1)                   |
| PLLA/CS/BO30 | 3226.5(188.6)                    | 20.9(4.4)                                 | 0.7(0.3)                   |

**Table 3.** Water vapor transmission rate (WVTR), Oxygen Permeability (OP), water sorption, and antioxidant activity values of all tested PLLA/CS and PLLA/CS/BO composite films.

| Code Name    | WVTR<br>(St. Dev.)<br>(g/m <sup>2</sup> ·day) | OP<br>(St. Dev.)<br>cm <sup>3</sup> ·mm/m <sup>2</sup> ·day | % Water Sorption<br>(St. Dev.) | Antioxidant Activity<br>after 24 h<br>(St. Dev.) |
|--------------|---|---|--------------------------------|--|
| PLLA         | 13.80(3.5)                                    | 541.6(2.4)  | 1.85(0.22)                     | n.d.   |
| PLLA/CS5     | 14.2(2.8)                                     | 538.7(2.8)  | 2.92(0.25)                     | 2.6(0.9)   |
| PLLA/CS10    | 16.3(3.1)                                     | 548.3(3.5)  | 5.04(1.65)                     | 5.8(1.2)   |
| PLLA/CS20    | 24.4(3.4)                                     | 569.5(4.3)  | 9.23(1.55)                     | 11.3(1.4)  |
| PLLA/CS30    | 35.1(3.8)                                     | 586.4(5.2)  | 26.57(2.96)                    | 16.4(1.5)  |
| PLLA/CS/BO5  | 12.74(2.5)                                    | 468.2(1.5)  | 1.81(0.35)                     | 7.8(0.9)   |
| PLLA/CS/BO10 | 13.54(3.2)                                    | 518.5(2.1)  | 1.94(1.75)                     | 12.8(1.2)  |
| PLLA/CS/BO20 | 20.22(2.8)                                    | 552.7(2.9)  | 6.23(1.85)                     | 24.4(1.4)  |
| PLLA/CS/BO30 | 30.41(4.2)                                    | 562.4(3.5)  | 20.57(2.86)                    | 34.6(1.5)  |

### 3. Results

#### 3.1. XRD Analysis

Figure 2 presents the XRD plots of the PLLA/CS and the PLLA/CS/BO films as well as of the “blank” PLLA film. The most intense diffraction peaks of the XRD measurement of the PLLA film is at  $2\theta$  values of  $16.6^\circ$  and  $18.96^\circ$ . This result is in agreement with previous reports [24,25]. By increasing the CS and CS/BO contents in the PLLA/CS and PLLA/CS/BO mixtures, the corresponding PLLA characteristic peaks of the FT-IR plots are decreased and shifted in smaller angles. Moreover, at a more careful glance, it is observed that the characteristic broad peak of CS at around  $20^\circ$  is increased by increasing the CS and CS/BO contents. These observations indicate effective blending of the PLLA chains with both the CS and CS/BO blends.

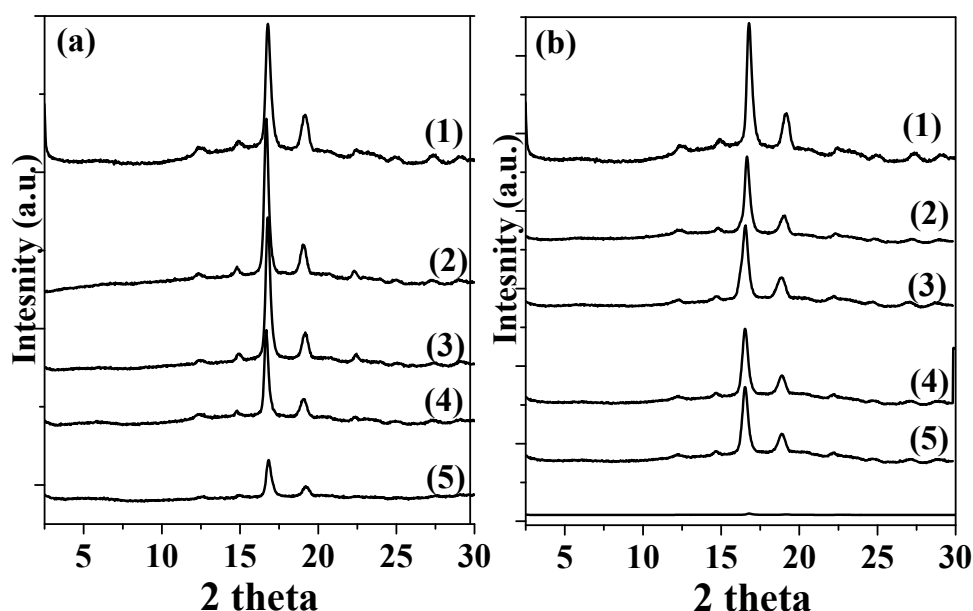


**Figure 2.** XRD plots of (a) (2) PLLA/CS5, (3) PLLA/CS10, (4) PLLA/CS20, and (5) PLLA/CS30 as well as (b) (2) PLLA/CS/BO5, (3) PLLA/CS/BO10, (4) PLLA/CS/BO20, and (5) PLLA/CS/BO30: in the upper part of both graphs (line (1)) is the corresponding “blank” PLLA XRD plot for comparison.



### 3.2. FT-IR

Figure 3 presents the FT-IR spectra of the PLLA/CS and the PLLA/CS/BO films as well as the FT-IR spectra of the “blank” PLLA film. Figure 3c presents the magnified spectra of the PLLA, PLLA/CS30, and PLLA/CS/BO30 films. The main characteristic peaks of both the PLLA and the CS material are observed in all spectra. For the PLLA/CS/BO30 film (see Figure 3c, spectrum (3)), the band at approximately  $1511\text{ cm}^{-1}$  can be attributed to the BO vibrations [20] and indicates effective mixing of the CS/BO blend with the PLLA chains. As it is denoted with the dot lines (see Figure 3a–c), the OH stretch band of the PLLA is presented at the wavenumber value  $3510\text{ cm}^{-1}$ . At wavenumber values of  $2941$  and  $2993\text{ cm}^{-1}$ , the CH and  $\text{CH}_3$  stretching bands are visible, whereas the characteristic band of the CO ester group is observed at  $1750\text{ cm}^{-1}$  [26].

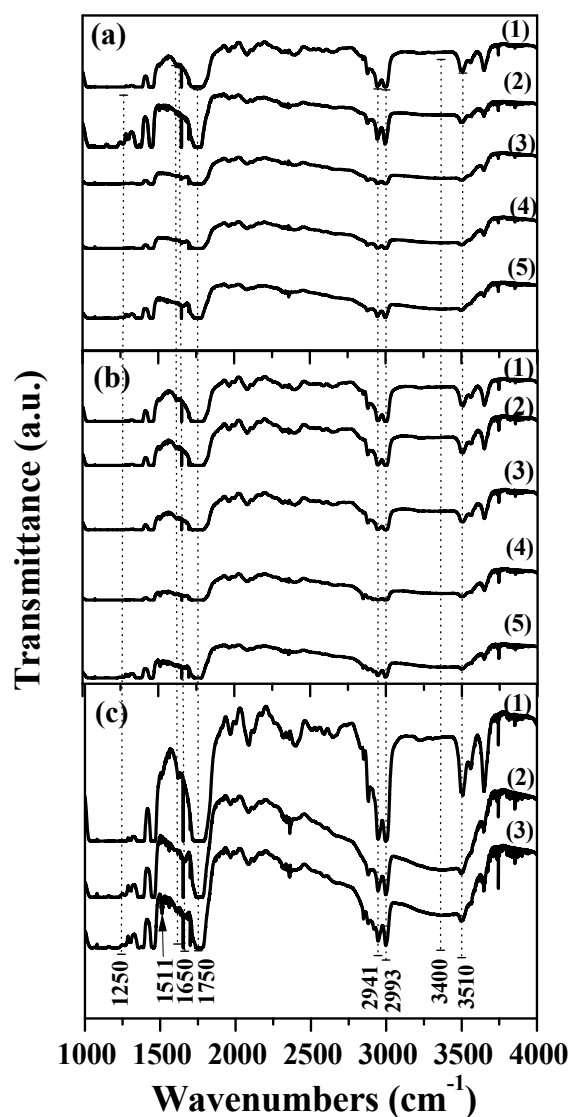


**Figure 3.** FT-IR spectra plots of (a) (1) PLLA (2) PLLA/CS5, (3) PLLA/CS10, (4) PLLA/CS20, and (5) PLLA/CS30; (b) (1) PLLA (2) PLLA/CS/BO5, (3) PLLA/CS/BO10, (4) PLLA/CS/BO20, and (5) PLLA/CS/BO30; and (c) (1) PLLA, (2) PLLA/CS30, and (3) PLLA/CS/BO30.

Furthermore, the broadband at the wavenumber value around  $3400\text{ cm}^{-1}$  corresponds to the OH and NH stretch of CS. For the CS material, the band at the wavenumber value  $1650\text{ cm}^{-1}$  corresponds to the amide I band. On the other hand, the amide III band [26,27] was not detected. This happens probably because of the low transmittance of the films in the wavenumber range  $1050\text{--}1300\text{ cm}^{-1}$ . By increasing the CS and the CS/BO contents in

the PLLA/CS and PLLA/CS/BO films, the characteristic peaks of the FT-IR plots, which correspond to the PLLA material, decreased. This fact indicated effective blending of the PLLA chains with the CS chains and the CS/BO blend. Furthermore, no PLLA peak shift is observed in PLLA/CS or in PLLA/CS/BO films. This fact indicates that no interaction exists between PLLA and CS chemical groups [28].

### 3.3. TG-DTA

Figure 4a shows the TG plots for pure PLLA and CS and for all the PLLA/CS blends. Figure 4b shows the TG plots for pure PLLA and CS/BO and for all the PLLA/CS/BO blends. Pure CS (see Figure 4a) and the CS/BO blend (see Figure 4b) exhibit two weight-loss steps. The first weight-loss step starts at around 100 °C and ends at around 200 °C and occurs due to elimination of the adsorbed moisture. The second weight-loss step starts at approximately 230 °C, ends at approximately 550 °C, and occurs because of decomposition of the CS chains [29]. Thus, the modification of CS with BO does not cause remarkable changes to the thermal behavior of the obtained CS/BO blend.

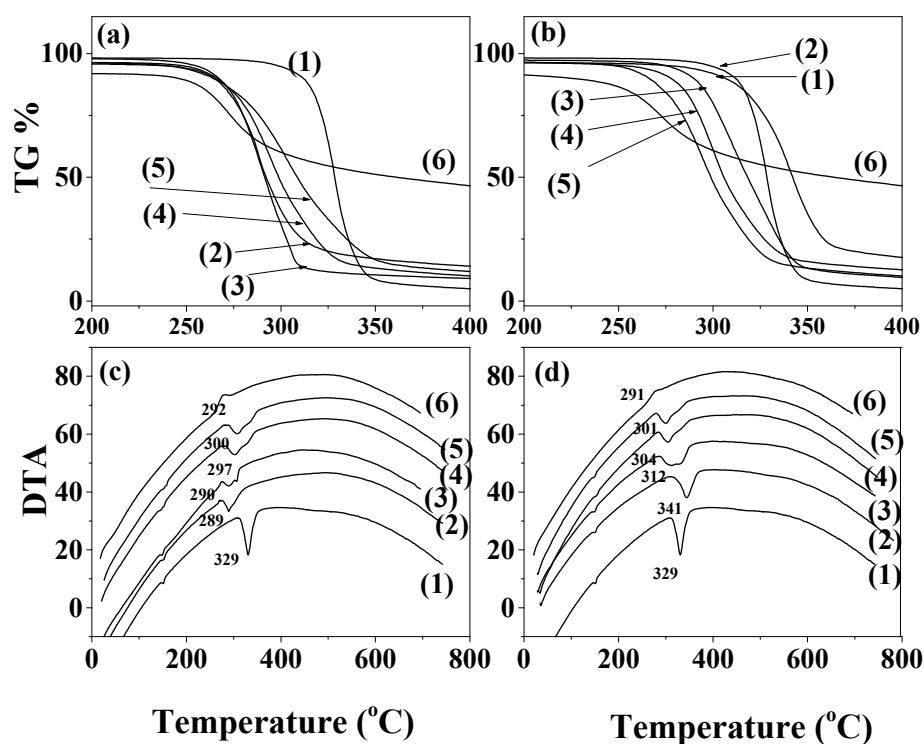


**Figure 4.** Thermogravimetric (TG) (a,b) and Differential Thermal Analysis (DTA) (c,d) plots of all PLLA/CS (a,c) and PLLA/CS/BO composite films as well as blank PLLA film, and pure CS and modified CS/BO powders: in Figure 4a,c (1) PLLA, (2) PLLA/CS5, (3) PLLA/CS10, (4) PLLA/CS20, (5) PLLA/CS30, and (6) CS are shown, and in Figure 4b,d, (1) PLLA, (2) PLLA/CS/BO5, (3) PLLA/CS/BO10, (4) PLLA/CS/BO20, (5) PLLA/CS/BO30, and (6) CS/BO are shown.

The TG plot of the pure PLLA (see Figure 4a,b line 1) shows one weight-loss step, which starts at around 310 °C [28,30]. Incorporation of pure CS in the PLLA chains causes a decrease in the decomposition temperature compared to that of the pure PLLA. After such mixing, the decomposition starting step occurs at lower temperature values. The same observation occurs in cases of 10%wt, 20%wt, and 30%wt CS/BO loading in the PLLA matrix. On the contrary, the incorporation of 5%wt of the CS/BO blend in the PLLA matrix shifts the decomposition temperature to higher values. These decomposition temperatures are better depicted in the DTA plots of the PLLA/CS samples (see Figure 4c) and the PLLA/CS/BO samples (see Figure 4d). According to these values, the PLLA/CS/BO films exhibit higher thermal stability than the corresponding PLLA/CS



films. The PLLA/CS/BO5 sample exhibits the highest decomposition temperature value, which is also higher than that of the “blank” PLLA film. Concluding, we could say that the thermogravimetric analysis experiments showed an enhancement of the thermal stability of the PLLA/CS/BO composite films compared to the thermal stability of the PLLA/CS composite films. The PLLA/CS/BO films with a composition of 5%w/w CS/BO blend in the PLLA matrix exhibited the highest thermal stability.

### 3.4. Tensile Properties

Figure 5a,b shows the stress–strain curves of the PLLA/CS and the PLLA/CS/BO composite films correspondingly. The average value, the standard deviation of Young's Modulus ( $E$ ) as well as of the tensile strength ( $\sigma_{\text{uts}}$ ), and the elongation at break ( $\epsilon_b$ ) were calculated. The results are presented in Table 2. A decrease in Young's Modulus and in tensile strength, and the elongation at break values are observed for all the PLLA/CS films compared to the respective values of the “blank” PLLA films. More specifically, as the CS content increased in the PLLA/CS films, the obtained Young's Modulus, the tensile strength, and the elongation at break values decreased further. This result is consistent with previous reports where the CS was blended with PLLA [9,11]. This happens because mixing of the thermoplastic polymer PLLA and CS is thermodynamically prohibited. Moreover, the two polymers are inherently incompatible [11,27].

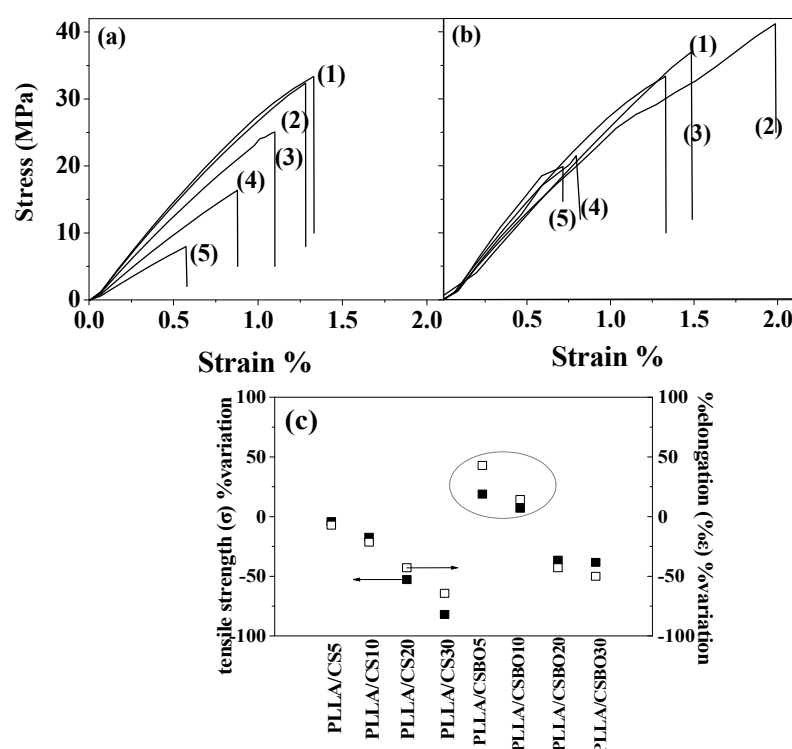


**Figure 5.** Strain–stress curves of (a) (1) PLLA, (2) PLLA/CS5, (3) PLLA/CS10, (4) PLLA/CS20, and (5) PLLA/CS30 and (b) (1) PLLA, (2) PLLA/CS/BO5, (3) PLLA/CS/BO10, (4) PLLA/CS/BO20, and (5) PLLA/CS/BO30, and (c) %variation of tensile strength ( $\sigma$ ) values and %elongation at break—( $\epsilon$ ) values are for all tested PLLA/CS and PLLA/CS/BO active packaging films.

On the contrary, the modified CS/BO blend exhibited better compatibility with PLLA. For PLLA/CS/BO5 and PLLA/CS/BO10 films (see Table 2), higher values of Young's Modulus, tensile strength, and elongation at break were obtained compared to the respective values of the “blank” PLLA films. Comparing the mechanical properties of the PLLA/CS/BO20 and the PLLA/CS/BO30 films with the relevant properties of the “blank” PLLA film, Young's Modulus values are still higher but the tensile strength and the elongation at break values decreased. To the best of our knowledge, it is the first reference

that PLLA/CS blends exhibit enhanced tensile strength and elongation at break values. This result is illustrated better in Figure 5c, where the %variation of tensile strength and elongation at break values of all PLLA/CS, PLLA/CS/BO, and “blank” PLLA films are plotted. From this figure, it is obvious that the CS/BO blends exhibited higher compatibility with the PLLA matrix in the cases of 5%w/w and 10%w/w nominal concentrations. This result indicates the use of the novel CS/BO blend as a compatibilizer agent.

### 3.5. Water Sorption

Calculated water sorption values are listed in Table 3. The addition of both CS and CS/BO in the PLLA matrixes increased the water sorption values because of the higher hydrophilicity of CS [9,11]. Hydrophobic modification of the CS with BO led to lower water sorption values for PLLA/CS/BO films as compared to the respective water sorption values of the PLLA/CS films. The lowest water sorption values were obtained for the PLLA/CS/BO5 and PLLA/CS/BO10 samples.

### 3.6. Water Barrier Properties

Calculated WVTR values are shown in Table 3. The PLLA/CS films exhibited higher WVTR values than the “blank” PLLA film, which is consistent with previous studies, [9,11]. This phenomenon is caused by the greater hydrophilicity of CS, which allows the diffusion of water molecules through the film. As the CS content increased, the WVTR values of the obtained PLLA/CS films increased further. On the contrary, the PLLA/CS/BO films exhibited lower WVTR values than the PLLA/CS films. The hydrophobic behavior of the BO makes the PLLA/CS/BO5 and PLLA/CS/BO10 films show lower WVTR values compared to the “blank” PLLA film. This result indicates that the hydrophobicity of the CS/BO blend prevails over the hydrophilicity of the pure CS material. This is supported by the TG and FTIR experiments which were discussed above. Thus, the BO in the modified CS/BO blend acts as a compatibilizer between the PLLA and the CS chains. Moreover, it acts as a hydrophobic barrier agent.

### 3.7. Oxygen Permeability (OP)

The calculated OP values for all the tested PLLA/CS, PLLA/CS/BO, and “blank” PLLA samples are listed in Table 3. The OP values exhibited a similar trend to that of the WVTR values. The PLLA/CS/BO films exhibited lower OP values than the PLLA/CS films. This result indicates that CS modification with BO led to more effective blending of the CS/BO blend with the PLLA matrix. Furthermore, it enhances the tortuosity of paths which are followed by the oxygen molecules inside the PLLA/CS/BO composite matrix. The PLLA/CS/BO5 and PLLA/CS/BO10 samples exhibited lower OP values compared to the respective values of the PLLA film.

This result in combination with the WVTR values and the % water sorption values could support the conclusion that 5%wt and 10%w/w CS/BO loading is optimal for such PLLA/CS/BO composite films.

### 3.8. Antioxidant Activity

Antioxidant activity values for the tested composite films are listed in Table 3. Considering the PLLA/CS films, such values were found to increase when the CS content increased. The PLLA/CS5 material exhibited values around 7.8%, the PLLA/CS10 exhibited values around 12.8%, and the PLLA/CS20 as well as the PLLA/CS30 exhibited values around 16.4%. It is known [30] that CS inhibits reactive oxygen species and prevents lipid oxidation of food. Antioxidant activity values increased further when the CS/BO blend was added to the PLLA matrix. The antioxidant activity values in such cases were around 2.6% for PLLA/CS5, around 5.8% for PLLA/CS10, around 24.4% for the PLLA/CS20, and around 34.6% for the PLLA/CS30 sample. This result indicates successful use of the BO molecules as an antioxidant agent in the modified CS/BO blend.

### 3.9. Statistical Analysis of the Experimental Data

All the experimental data, i.e.,  $E$ ,  $\sigma_{\text{uts}}$ ,  $\% \epsilon$ , WVP, % water sorption, OP, and % antioxidant activity after 24 h, were statistically treated using the statistical software SPSS, IBM, Chicago, IL, USA, ver. 20. More specifically, for all statistical tests, we assumed a confidence interval (C.I.) of 95%, which is the most common value used for such analyses. Thus, the value of the statistical significance level is  $p = 0.05$ . The results for mean values and standard deviation of the abovementioned parameters are presented in Tables 2 and 3.

Furthermore, for each one of the abovementioned properties, the hypothesis  $H_0$  (mean values could be assumed as equal) was examined for all the combinations of samples. This was performed for supporting the hypothesis that, considering different samples, every property has a statistically different mean value. The normality tests for data sets indicated that some of them cannot be assumed as normal distributions. Also, variance homogeneity tests, according to Levene's criterion, showed that, in some cases of films, we did not have homogeneity of variance. Thus, we could not use the ANOVA method for testing the mean equalities. Instead, we used the nonparametric Kruskal–Wallis method. The results are presented in Table 4. The (*Sig.*) values which are presented in this table were compared with the significance level ( $p$ ). It is obvious from these comparisons that, in all cases, the (*Sig.*) values are smaller than the significance level ( $p$ ) values. Thus, in all cases and for all parameters, mean values are statistically different. The smaller the (*Sig.*) value, compared to significance level value ( $p$ ), the more assured that the mean values are statistically unequal. For *Sig.* = 0, the inequality of means is 100% statistically assured. For (*Sig.*) close to ( $p$ ) values, the inequality of means is limitedly assured. According to the clarifications mentioned above, we developed the empirical Equation (3) for calculation of an empirical factor we call “inequality assurance” (*IA*). This factor is the percentage of deviation of (*Sig.*) from ( $p$ ) values toward 0. The “inequality assurance” (*IA*) is calculated as follows:

$$IA = \frac{p - \text{Sig.}}{p} * 100 \quad (3)$$

It is obvious from Table 4 that, in all cases, the inequality of mean values is statistically assured strongly ( $IA \geq 88\%$ ).

**Table 4.** Mean values inequality test of modulus of elasticity ( $E$ ), tensile strength ( $\sigma_{\text{uts}}$ ), % elongation at break ( $\epsilon_b$ ), water vapor permeability WVTR, % water sorption, oxygen permeability (OP), and % antioxidant activity after 24 h of all tested films.

|                                   | <i>Sig.</i> | <i>IA</i> |
|-----------------------------------|-------------|-----------|
| $E$                               | 0.002       | 96        |
| $\Sigma_{\text{uts}}$             | 0.005       | 90        |
| $\% \epsilon$                     | 0.003       | 94        |
| WVTR                              | 0.005       | 90        |
| % water sorption                  | 0.005       | 90        |
| OP                                | 0.004       | 92        |
| % Antioxidant activity after 24 h | 0.001       | 98        |

## 4. Conclusions

Following the spirit of cyclic economy in this work, we developed a fully bio-based and biodegradable active packaging film using the fully biodegradable PLLA polymer in combination with a by-product of the food industry, i.e., chitosan (CS), and a natural antioxidant, i.e., the basil-oil extract (BO). Concluding the previous analysis, we could say that the modification of CS with BO molecules via a “green” adsorption/desorption process leads successfully to a novel hydrophobic CS/BO bioactive blend which could be used as a masterbatch in extrusion molding processes. The development of PLLA/CS/BO active packaging films exhibits enhanced tensile, barrier, and antioxidant properties. The most promising films in this work were the composite PLLA films loaded with a CS/BO blend in compositions from 5%w/w to 10%w/w. The last films showed enhanced tensile

properties, the lowest % water sorption, enhanced water/oxygen barrier properties, and significant antioxidant activity. According to these results, the composite PLLA/CS/BO5 and PLLA/CS/BO10 films could be novel, promising, active packaging films. Moreover, the novel and promising results of this study could be used as a guide for the encapsulation of other EOs in such PLLA/CS films with more improved characteristics.

**Author Contributions:** Conceptualization, C.E.S., A.E.G., and M.A.K.; methodology, C.E.S., A.E.G., and M.A.K.; validation, C.E.S., A.E.G., M.A.K., M.B., and A.L.; formal analysis, C.E.S., A.E.G., M.A.K., M.B., and A.L.; investigation, C.E.S., A.E.G., M.A.K., M.B., A.L., and Z.S.; resources, C.E.S., A.E.G., M.A.K., M.B., A.L., and Z.S.; data curation, C.E.S., A.E.G., M.A.K.; M.B., A.L., and Z.S., writing—original draft preparation, C.E.S., A.E.G., and M.A.K.; writing—review and editing, C.E.S., A.E.G., and M.A.K.; visualization, C.E.S., A.E.G., and M.A.K.; supervision, C.E.S., A.E.G., and M.A.K.; and project administration, C.E.S., A.E.G., and M.A.K. All authors have read and agreed to the published version of the manuscript.

**Funding:** This research received no external funding.

**Institutional Review Board Statement:** Not applicable.

**Informed Consent Statement:** Not applicable.

**Data Availability Statement:** Not applicable.

**Conflicts of Interest:** The authors declare no conflict of interest.

## References

- John, R.P.; Nampoothiri, K.M.; Pandey, A. Fermentative production of lactic acid from biomass: An overview on process developments and future perspectives. *Appl. Microbiol. Biotechnol.* **2007**, *74*, 524–534. [\[CrossRef\]](#) [\[PubMed\]](#)
- Connolly, M.; Zhang, Y.; Brown, D.M.; Ortuño, N.; Jordá-Beneyto, M.; Stone, V.; Fernandes, T.F.; Johnston, H.J. Novel polylactic acid (PLA)-organoclay nanocomposite bio-packaging for the cosmetic industry; migration studies and in vitro assessment of the dermal toxicity of migration extracts. *Polym. Degrad. Stab.* **2019**, *168*, 108938. [\[CrossRef\]](#)
- Rasal, R.M.; Janorkar, A.V.; Hirt, D.E. Poly(lactic acid) modifications. *Prog. Polym. Sci.* **2010**, *35*, 338–356. [\[CrossRef\]](#)
- Ghorpade, V.M.; Gennadios, A.; Hanna, M.A. Laboratory composting of extruded poly(lactic acid) sheets. *Bioresour. Technol.* **2001**, *76*, 57–61. [\[CrossRef\]](#)
- Neumann, I.A.; Flores-Sahagun, T.H.S.; Ribeiro, A.M. Biodegradable poly (l-lactic acid) (PLLA) and PLLA-3-arm blend membranes: The use of PLLA-3-arm as a plasticizer. *Polym. Test.* **2017**, *60*, 84–93. [\[CrossRef\]](#)
- Gerometta, M.; Rocca-Smith, J.R.; Domenech, S.; Karbowiak, T. Physical and Chemical Stability of PLA in Food Packaging. In *Reference Module in Food Science*; Elsevier: Amsterdam, The Netherlands, 2019; ISBN 978-0-08-100596-5.
- Muzzarelli, R.A.A.; Boudrant, J.; Meyer, D.; Manno, N.; Demarchis, M.; Paoletti, M.G. Current views on fungal chitin / chitosan, human chitinases, food preservation, glucans, pectins and inulin: A tribute to Henri Braconnot, precursor of the carbohydrate polymers science, on the chitin bicentennial. *Carbohydr. Polym.* **2012**, *87*, 995–1012. [\[CrossRef\]](#)
- Cazón, P.; Vázquez, M. Applications of Chitosan as Food Packaging Materials. In *Sustainable Agriculture Reviews 36: Chitin and Chitosan: Applications in Food, Agriculture, Pharmacy, Medicine and Wastewater Treatment*; Crini, G., Lichtfouse, E., Eds.; Sustainable Agriculture Reviews; Springer International Publishing: Cham, Switzerland, 2019; pp. 81–123, ISBN 978-3-030-16581-9.
- Bonilla, J.; Fortunati, E.; Vargas, M.; Chiralt, A.; Kenny, J.M. Effects of chitosan on the physicochemical and antimicrobial properties of PLA films. *J. Food Eng.* **2013**, *119*, 236–243. [\[CrossRef\]](#)
- Stoleru, E.; Dumitriu, R.P.; Munteanu, B.S.; Zaharescu, T.; Tănase, E.E.; Mitelut, A.; Ailiesei, G.-L.; Vasile, C. Novel procedure to enhance PLA surface properties by chitosan irreversible immobilization. *Appl. Surf. Sci.* **2016**, *367*, 407–417. [\[CrossRef\]](#)
- Răpă, M.; Mitelut, A.C.; Tănase, E.E.; Grosu, E.; Popescu, P.; Popa, M.E.; Rosnes, J.T.; Sivertsvik, M.; Darie-Niță, R.N.; Vasile, C. Influence of chitosan on mechanical, thermal, barrier and antimicrobial properties of PLA-biocomposites for food packaging. *Compos. Part. B Eng.* **2016**, *102*, 112–121. [\[CrossRef\]](#)
- Claro, P.I.C.; Neto, A.R.S.; Bibbo, A.C.C.; Mattoso, L.H.C.; Bastos, M.S.R.; Marconcini, J.M. Biodegradable Blends with Potential Use in Packaging: A Comparison of PLA/Chitosan and PLA/Cellulose Acetate Films. *J. Polym. Environ.* **2016**, *24*, 363–371. [\[CrossRef\]](#)
- Fathima, P.E.; Panda, S.K.; Ashraf, P.M.; Varghese, T.O.; Bindu, J. Polylactic acid/chitosan films for packaging of Indian white prawn (*Fenneropenaeus indicus*). *Int. J. Biol. Macromol.* **2018**, *117*, 1002–1010. [\[CrossRef\]](#) [\[PubMed\]](#)
- Ye, J.; Wang, S.; Lan, W.; Qin, W.; Liu, Y. Preparation and properties of polylactic acid-tea polyphenol-chitosan composite membranes. *Int. J. Biol. Macromol.* **2018**, *117*, 632–639. [\[CrossRef\]](#) [\[PubMed\]](#)
- Kasirajan, S.; Umapathy, D.; Chandrasekar, C.; Aafrin, V.; Jenitapeter, M.; Udhyaasooriyan, L.; Packirisamy, A.S.B.; Muthusamy, S. Preparation of poly(lactic acid) from *Prosopis juliflora* and incorporation of chitosan for packaging applications. *J. Biosci. Bioeng.* **2019**, *128*, 323–331. [\[CrossRef\]](#) [\[PubMed\]](#)

16. Sánchez-González, L.; Vargas, M.; González-Martínez, C.; Chiralt, A.; Cháfer, M. Use of Essential Oils in Bioactive Edible Coatings: A Review. *Food Eng. Rev.* **2011**, *3*, 1–16. [[CrossRef](#)]
17. Sanches-Silva, A.; Costa, D.; Albuquerque, T.G.; Buonocore, G.G.; Ramos, F.; Castilho, M.C.; Machado, A.V.; Costa, H.S. Trends in the use of natural antioxidants in active food packaging: A review. *Food Addit. Contam. Part. A* **2014**, *31*, 374–395. [[CrossRef](#)] [[PubMed](#)]
18. Salgado, P.R.; Di Giorgio, L.; Musso, Y.S.; Mauri, A.N. *Bioactive Packaging*; Elsevier Inc.: Amsterdam, The Netherlands, 2019; ISBN 978-0-12-814130-4.
19. Arroyo, B.J.; Santos, A.P.; de Melo, E.d.A.; Campos, A.; Lins, L.; Boyano-Orozco, L.C. Chapter 8—Bioactive Compounds and Their Potential Use as Ingredients for Food and Its Application in Food Packaging. In *Bioactive Compounds*; Campos, M.R.S., Ed.; Woodhead Publishing: Sawston, UK, 2019; pp. 143–156, ISBN 978-0-12-814774-0.
20. Giannakas, A.; Tsagkalias, I.; Achilias, D.S.; Ladavos, A. A novel method for the preparation of inorganic and organo-modified montmorillonite essential oil hybrids. *Appl. Clay Sci.* **2017**, *146*, 362–370. [[CrossRef](#)]
21. Giannakas, A.; Spanos, C.G.; Kourkouvelis, N.; Vaimakis, T.; Ladavos, A. Preparation, characterization and water barrier properties of PS/organo-montmorillonite nanocomposites. *Eur. Polym. J.* **2008**, *44*, 3915–3921. [[CrossRef](#)]
22. Giannakas, A.; Patsaoura, A.; Barkoula, N.-M.; Ladavos, A. A novel solution blending method for using olive oil and corn oil as plasticizers in chitosan based organoclay nanocomposites. *Carbohydr. Polym.* **2017**, *157*, 550–557. [[CrossRef](#)]
23. Grigoriadi, K.; Giannakas, A.; Ladavos, A.K.; Barkoula, N.-M. Interplay between processing and performance in chitosan-based clay nanocomposite films. *Polymer Bull.* **2015**, *72*. [[CrossRef](#)]
24. Wasanasuk, K.; Tashiro, K.; Hanesaka, M.; Ohhara, T.; Kurihara, K.; Kuroki, R.; Tamada, T.; Ozeki, T.; Kanamoto, T. Crystal Structure Analysis of Poly(L-lactic Acid)  $\alpha$  Form On the basis of the 2-Dimensional Wide-Angle Synchrotron X-ray and Neutron Diffraction Measurements. *Macromolecules* **2011**, *44*, 6441–6452. [[CrossRef](#)]
25. Hosen, M.S.; Rahaman, M.H.; Gafur, M.A.; Habib, R.; Qadir, M.R. Preparation and Characterization of Poly(L-lactic acid)/Chitosan/Microcrystalline Cellulose Blends. *Chem. Sci. Int. J.* **2017**, 1–10. [[CrossRef](#)]
26. Duarte, A.R.C.; Mano, J.F.; Reis, R.L. Novel 3D scaffolds of chitosan–PLLA blends for tissue engineering applications: Preparation and characterization. *J. Supercrit. Fluids* **2010**, *54*, 282–289. [[CrossRef](#)]
27. Giannakas, A.; Salmas, C.; Leontiou, A.; Tsimogiannis, D.; Oreopoulou, A.; Braouhli, J. Novel LDPE/Chitosan Rosemary and Melissa Extract Nanostructured Active Packaging Films. *Nanomaterials* **2019**, *9*, 1105. [[CrossRef](#)] [[PubMed](#)]
28. Sunilkumar, M.; Francis, T.; Thachil, E.T.; Sujith, A. Low density polyethylene–chitosan composites: A study based on biodegradation. *Chem. Eng. J.* **2012**, *204*, 114–124. [[CrossRef](#)]
29. Prasanna, K.; Sailaja, R.R.N. Blends of LDPE/chitosan using epoxy-functionalized LDPE as compatibilizer. *J. Appl. Polym. Sci.* **2012**, *124*, 3264–3275. [[CrossRef](#)]
30. Rajalakshmi, A.; Krithiga, N.; Jayachitra, A. Antioxidant Activity of the Chitosan Extracted from Shrimp Exoskeleton. *Middle East. J. Sci. Res.* **2013**, *16*, 1446–1451. [[CrossRef](#)]